



Supplementary Information for

Structural insights into membrane remodeling by SNX1

Yan Zhang, Xiaoyun Pang*, Jian Li, Jiashu Xu, Victor W. Hsu* and Fei Sun*

Corresponding authors: Xiaoyun Pang (pangxy@ibp.ac.cn), Victor Hsu (vhsu@bwh.harvard.edu) and Fei Sun (feisun@ibp.ac.cn).

This PDF file includes:

Figures S1 to S10
Tables S1
Legends for Movies S1

Other supplementary materials for this manuscript include the following:

Movies S1

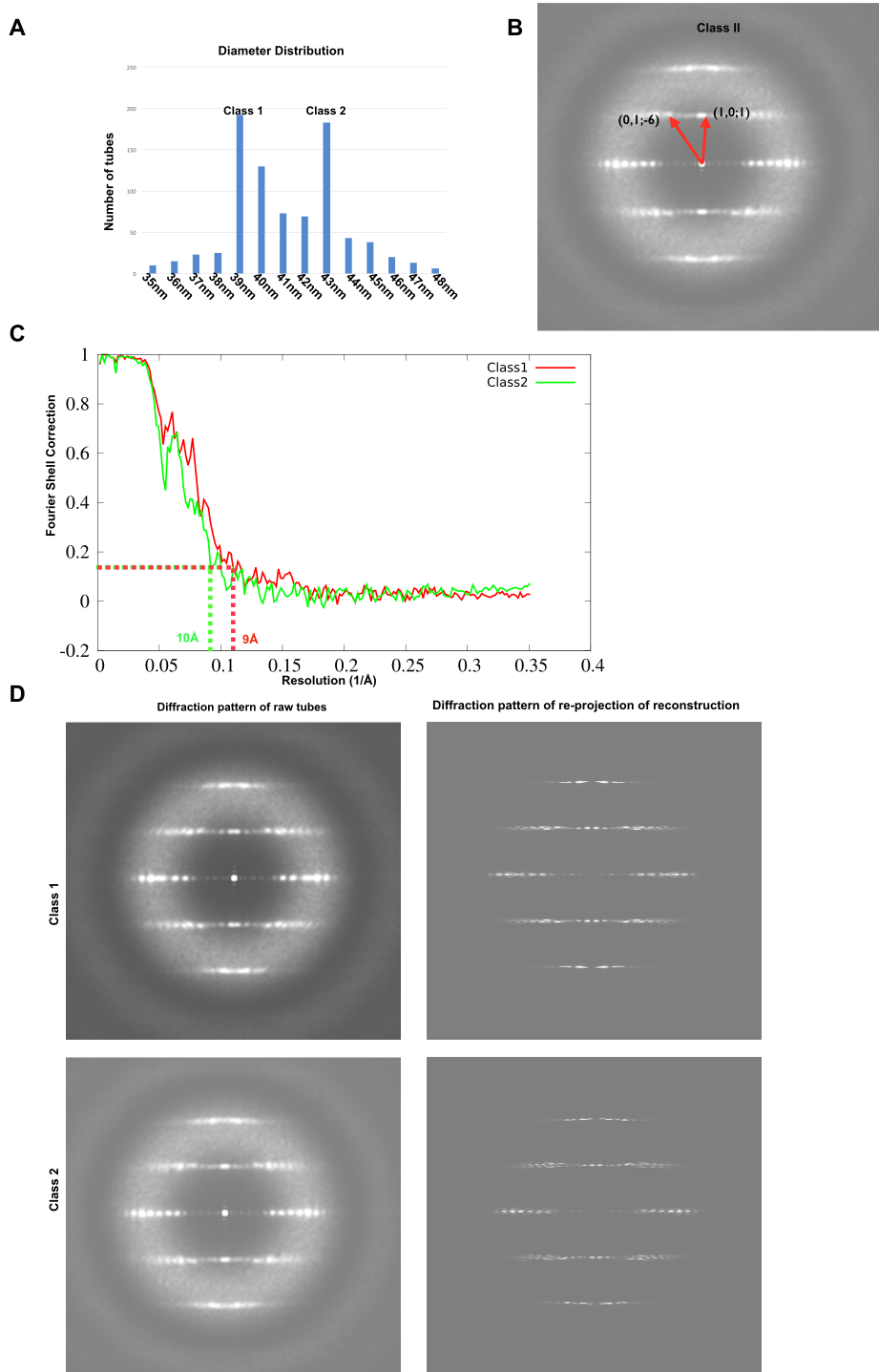


Fig. S1. Image processing of SNX1 membrane tubules. (A) Statistical histogram of the diameters of tubules generated by SNX1 in cryo-EM experiments, plotted as number of tubules versus tubule diameters (nm). (B) Average of helical diffraction patterns for tubules of class II. (C) The

FSC curves calculated between the helical reconstructed cryo-EM maps and the models for class I and class II respectively. The resolution is 9 Å for class I and 10 Å for class II with the cut-off 0.143. (D) Average of helical diffraction patterns for tubules (left) of class I and class II and projection of diffraction patterns of the final reconstructed maps (right) for Class I and II, respectively.

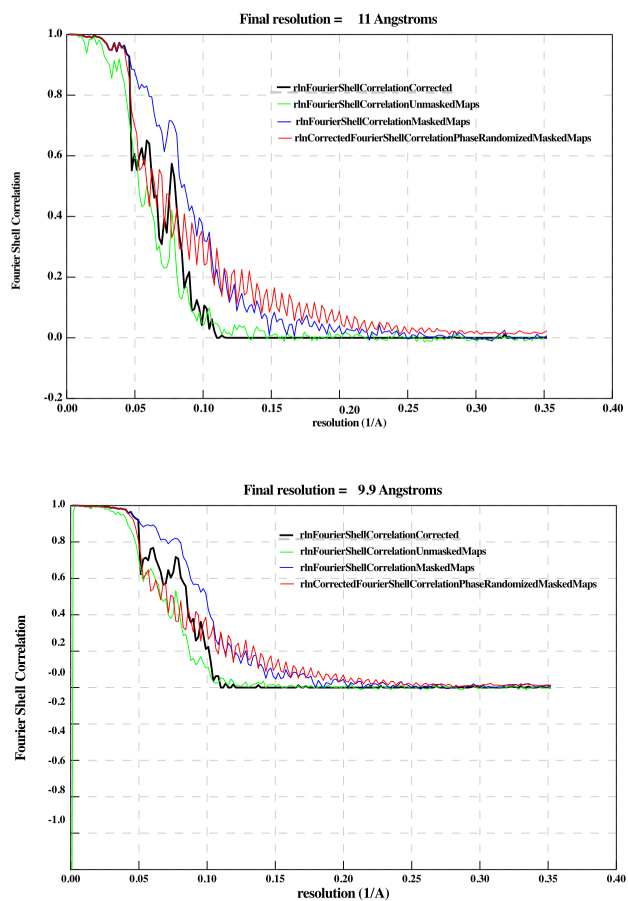


Fig. S2. FSC curves of Class I (top) and Class II (bottom) maps reconstructed by RELION3.0.

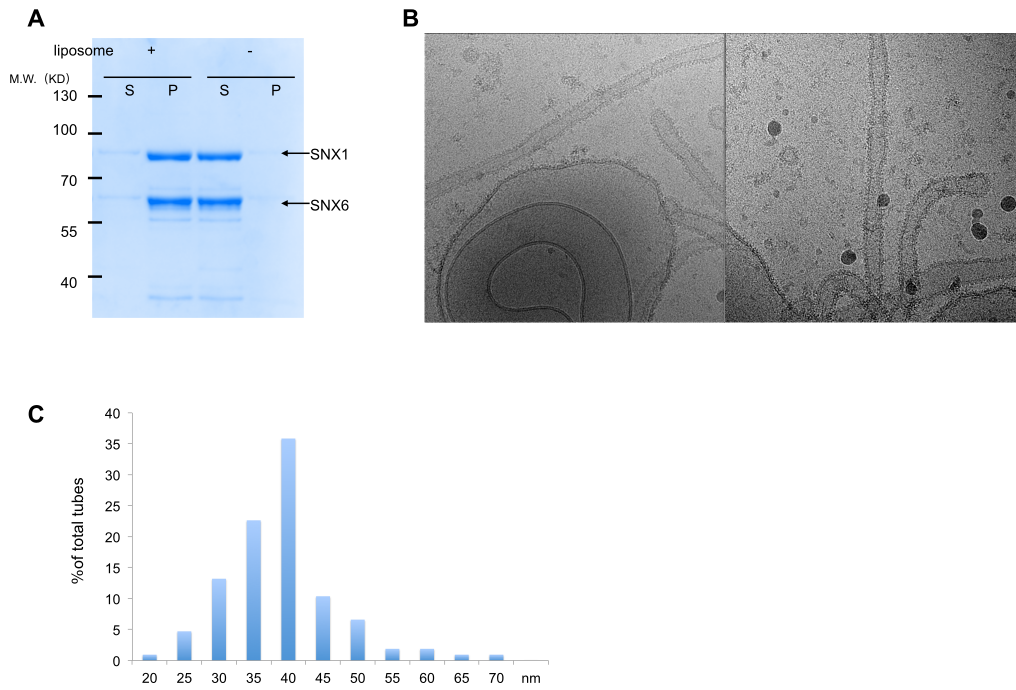


Fig. S3. Studies on the SNX1/SNX6 heterodimer. (A) Binding of SNX1/SNX6 to liposomes as assessed by the co-precipitation assay. S, supernatant, P, pellet. (B) Cryo-EM micrographs of tubules coated with the SNX1/SNX6 heterodimer. (C) Statistical histogram of the diameters of tubules induced by the SNX1/SNX6 heterodimer.

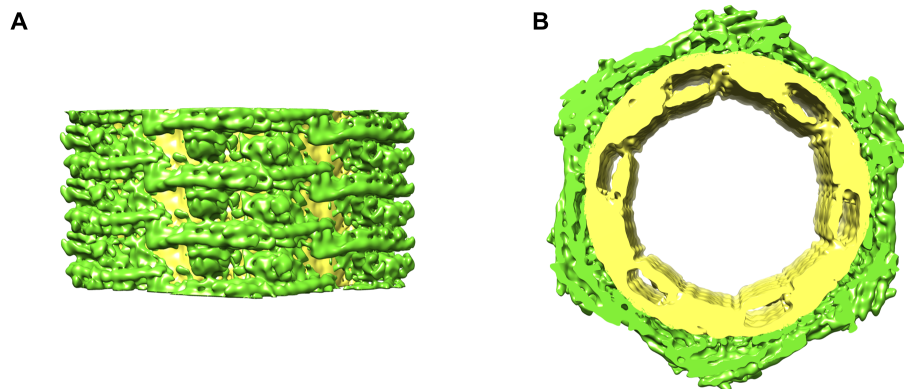


Fig. S4. Density map of SNX1 coated tubule of Class I with protein layer (green) and membrane layer (yellow) shown in differing contour levels. (A) Side view and (B) Top view. The contour level for the protein layer is 6.42 which discerns the secondary structural elements of SNX1, similar to that shown in Figure 2C, while the contour level for the membrane layer is reduced to 2.81 so that the membrane bilayer can be displayed as a continuous density.

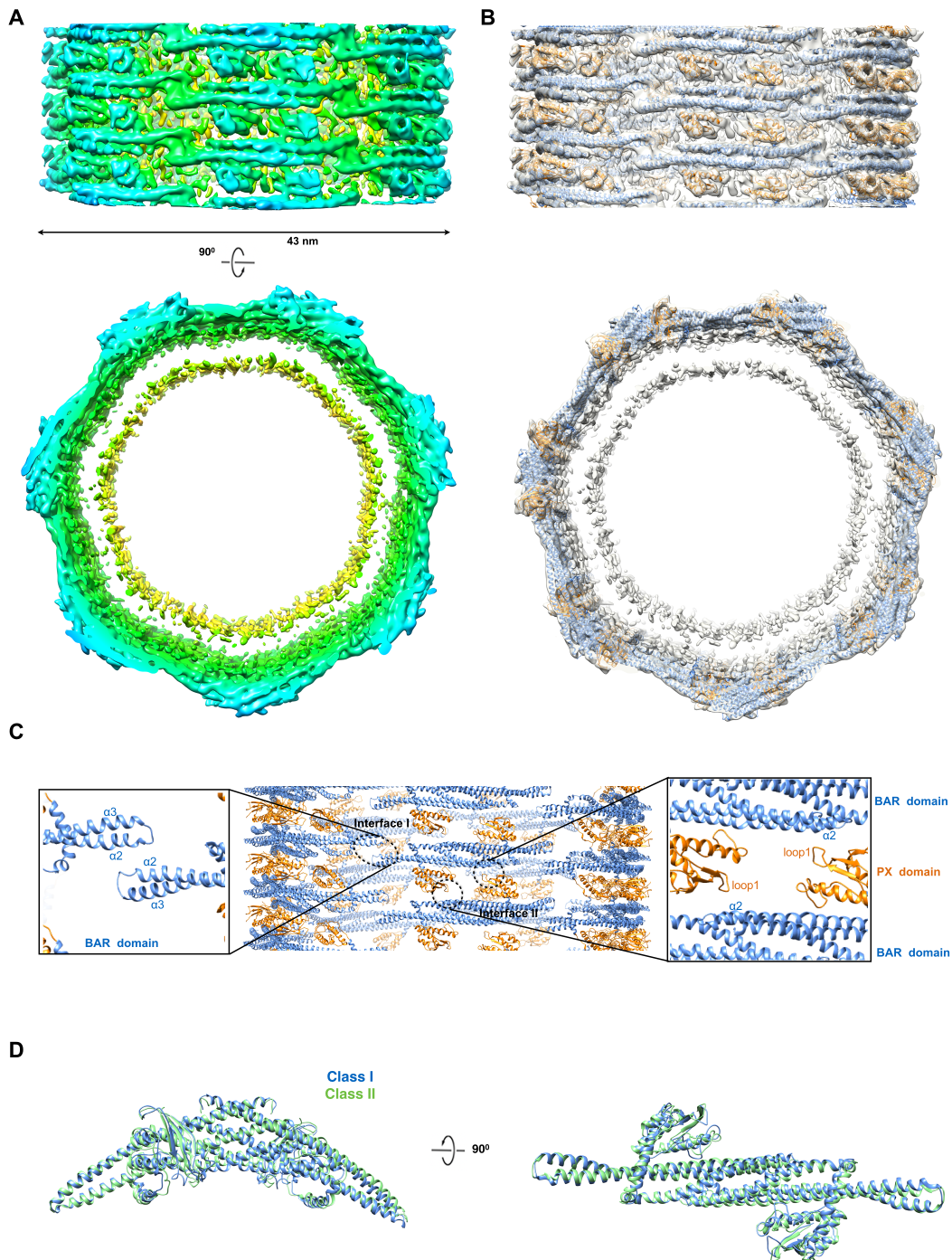


Fig. S5. 3D Reconstructions of class II tubules coated with SNX1. (A) Cryo-EM map of a class II tubule with the side view shown on top and the cross-section view shown on bottom. The map is colored according to the cylinder radius from red to blue. (B) The SNX1 structure in cartoon representation is fitted onto the EM map, with the PX domain colored in gold and the BAR domain

colored in blue. (C) Structural model of the SNX1 helical assembly for the class II tubules. Interface I and II are highlighted by dashed black circles. The zoom-in views of these regions are also shown. (D) Superimposing the SNX1 dimers from class I (blue) and class II (green) tubules.

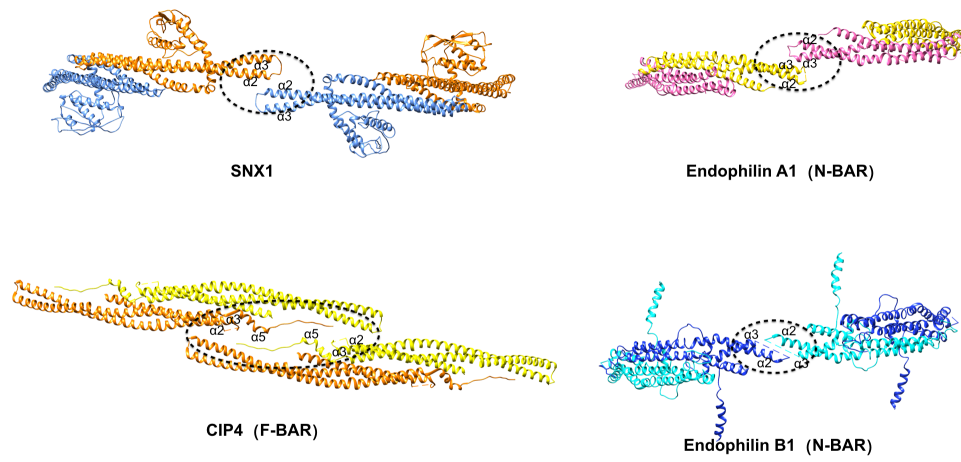
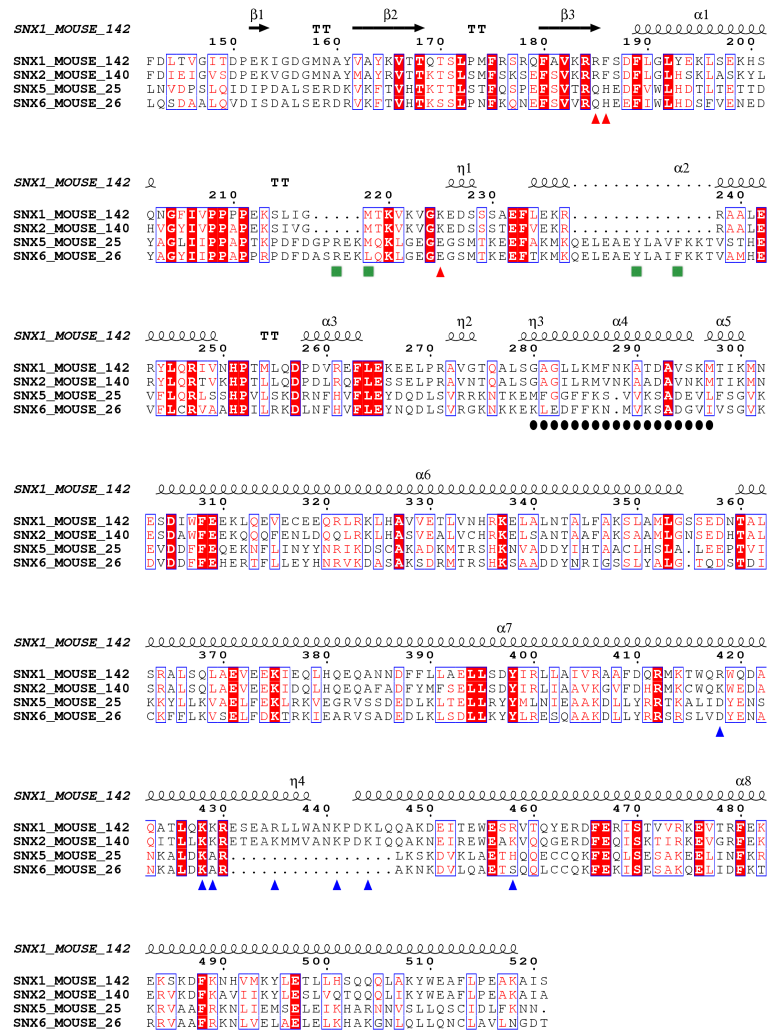


Fig. S6. Structural comparisons between cryo-EM structures of SNX1 and other BAR-containing proteins. The BAR domains of Endophilin A1 (PDB: 1ZWW) and Endophilin B1 (PDB: 6UP6) belong to the N-BAR subfamily, while the EFC domain of CIP4 (PDB: 2EFK and EMDB 1471) belongs to the F-BAR subfamily.

A



B

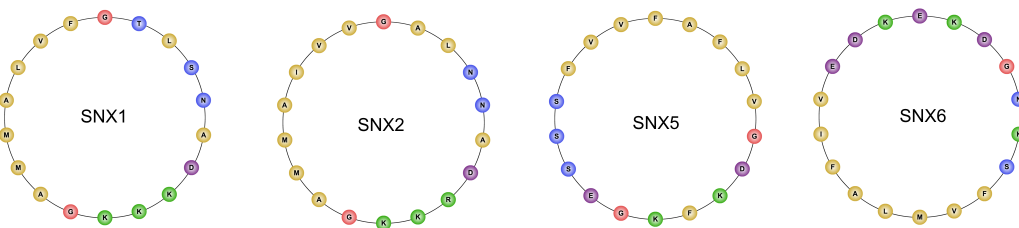


Fig. S7. Sequence analysis of SNX members. (A) Sequence alignment among SNX1, SNX2, SNX5 and SNX6. Strictly conserved residues are highlighted in red. Secondary structural elements of SNX1 are depicted at the top of the alignments. Cargo binding residues are labeled with green squares. The amphipathic helix is labeled with black circles. The PI3P binding residues are labeled with red triangles. The charged residues on the concave surface are labeled

with blue triangles. (B) Amphipathic helix analysis of SNX members using a helical wheel algorithm (http://www-nmr.cabm.rutgers.edu/bioinformatics/Proteomic_tools/Helical_wheel/).

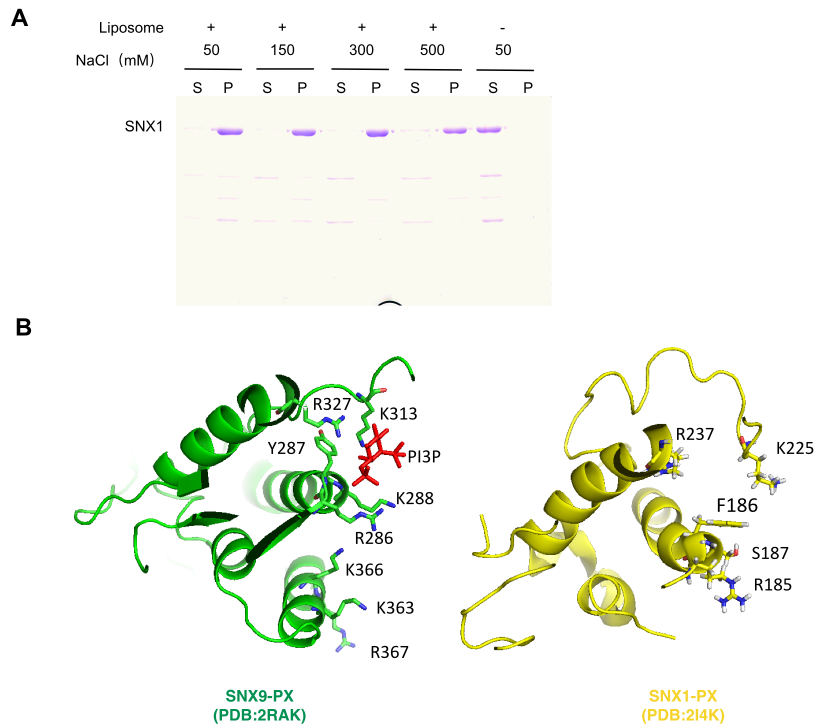


Fig. S8. Additional characterizations of SNX1. (A) Co-precipitation assay showing SNX1 binding to liposomes at different NaCl concentrations, S, supernatant, P, pellet. (B) Structure-based PI(3)P binding pocket analysis for SNX1(PDB 2I4K) and SNX9 (PDB 2RAK). Residues contacting the PI(3)P are shown and labeled.

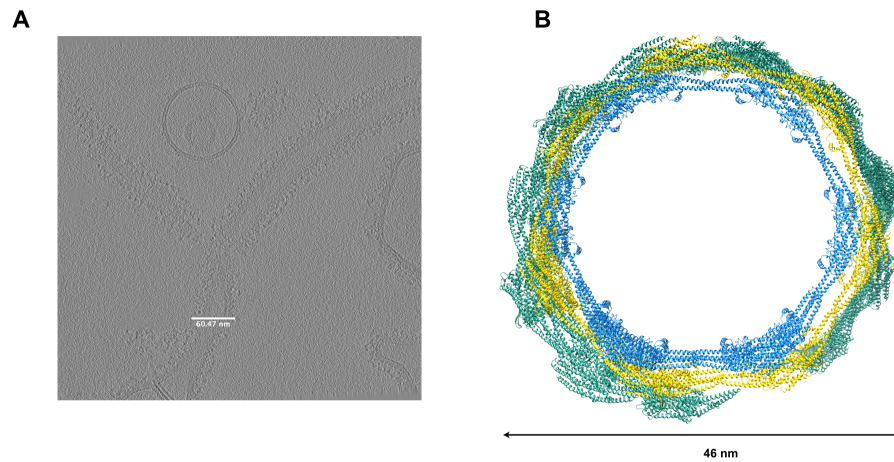


Fig. S9. Comparing the diameters of tubules coated by retromer-Vps5 complex versus by SNX1. (A) A slice of cryo-ET tomogram (EMDB-0163) showing tubule coated with the retromer-Vps5 complex. (B) A hypothetical model of a tubule coated by a Vps5 assembly (green) is superimposed onto the structural models of the SNX1 assembly from class I (blue) and class II (yellow) tubules.

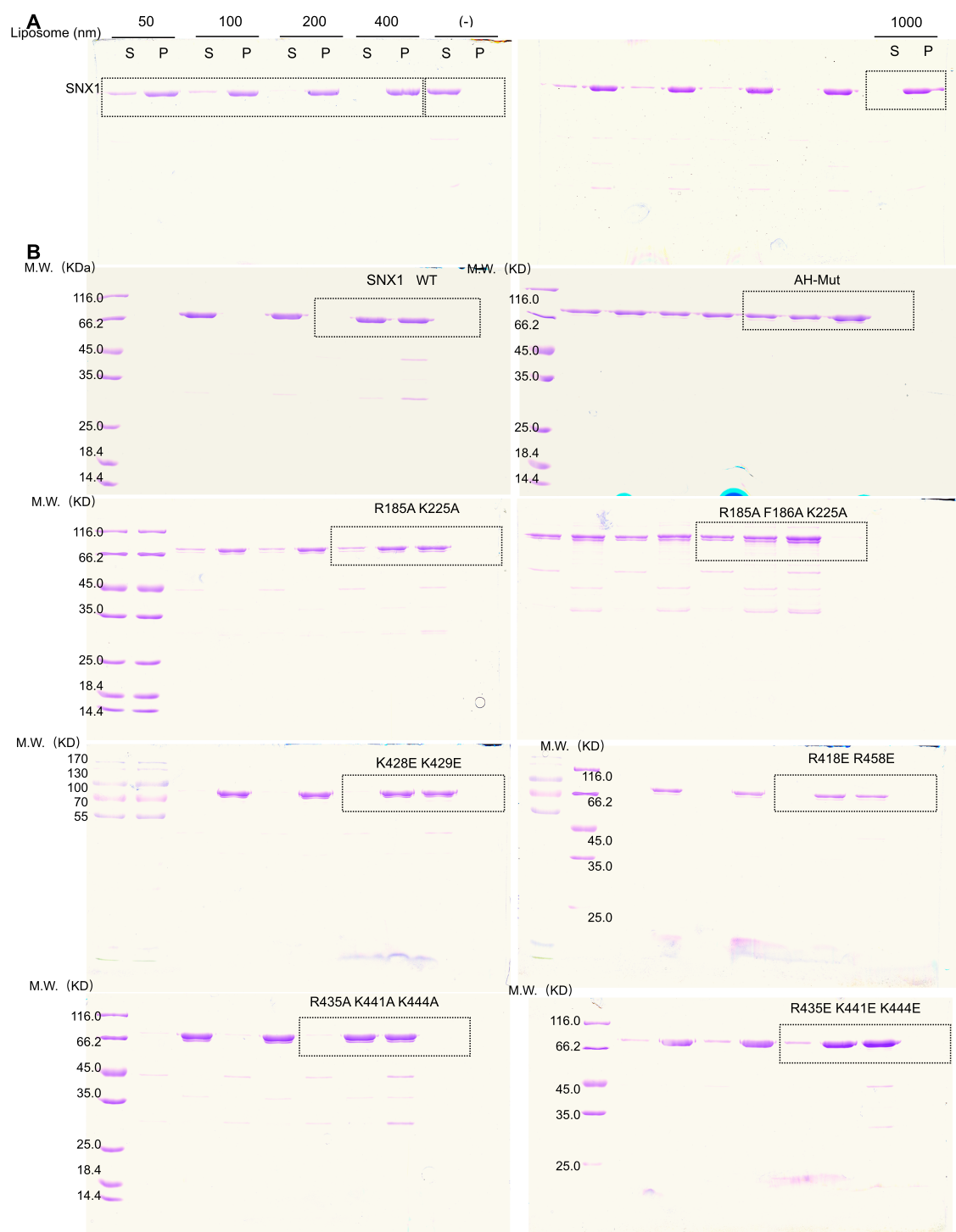


Fig. S10. Uncropped gel scans. (A) Binding of WT form of SNX1 to liposomes of varying sizes (as indicated) is assessed by the co-precipitation assays. (B) Binding of mutant forms of SNX1 (as indicated) to liposomes is assessed by the co-precipitation assay. S, supernatant, P, pellet.

Table S1. Data collection and refinement statistics.

Data collection		
Magnification	59000	
Voltage (kV)	300	
Microscope	Titan Krios	
Electron dose (e-/ Å ²)	~50	
Defocus range (µm)	(-0.5, -2.5)	
Camera	Falcon II	
Pixel size (Å)	1.42	
Software	Serial EM	
Helical reconstruction	Class I	Class II
Initial particle numbers	11,795	11,677
Final particle numbers	11,529	11,141
Resolution (Å)	9.0	10.0
Diameters (nm)	39	43
Subunits per turn	5.99	6.98
Pitch (Å)	52.3	52.6
Twist (°)	60.11	51.53
Rise (Å)	8.74	7.53

Movie S1. Structure of SNX1 coating on membrane.